Computational and Experimental Evaluation of Helicopter Rotor Tips for High-Speed Flight

Matthew T. Scott* and Dave Sigl†
Bell Helicopter Textron, Inc., Fort Worth, Texas 76101
and
Roger C. Strawn‡
NASA Ames Research Center, Moffett Field, California 94035

This paper describes a computational and experimental procedure for the evaluation of the helicopter rotor tips that exhibit properties providing improved performance in high-speed forward flight. The study uses an unsteady full-potential solver on the advancing side of the rotor disk, where transonic flight regimes dominate and the rotor blade is traditionally at low angles of attack. Computational results in the regime show that single- and double-swept planforms of constant t/c require less power than their rectangular counterparts at transonic flight conditions. Double-swept planforms such as those used by the British Experimental Rotor Program (BERP) tip exhibit the most favorable performance. Alteration of the t/c distribution through sectional taper results in further power reduction, and these benefits are compared with those acquired solely from the variation in planform. Simulations of the retreating blade fluid environment have been conducted in a wind tunnel with uninstrumented models of the blade tips. Forces and moments measured during angle-of-attack sweeps reveal the soft-stall phenomenon of the BERP planform as well as the delayed stall of the single-swept hyperbolic tip. Hot-wire anemometry and flow visualization techniques have been used to identify the structure of vortical and separated regions of each blade at each flight condition. Results show that double-swept tip shapes create counter-rotating vortices that augment the lifting capabilities of the blade at high angles of attack and delay the onset of stall. Analysis of the fluid mechanisms responsible for these results will enhance existing design methodology.

Nomenclature

a	= speed of sound
C_D, $C_D(x)$	= overall and sectional coefficient of drag, respectively
C_L, $C_L(x)$	= overall and sectional coefficient of lift, respectively
C_M, $C_M(x)$	= overall and sectional coefficient of moment (measured about the quarter chord), respectively
c_{root}	= chord length of the airfoil section at the inboard boundary of the computational zone
$c(x)$	= local chord length
$M_{rot_{tip}}$	= tip Mach number due solely to rotation
$\tilde{P}_{0_{tip}}$	= nondimensionalized power required to drive tip region
r/R	= radial blade station nondimensionalized by rotor radius (same as x)
α, $\alpha(x)$	= overall and sectional angles of attack, respectively
μ	= rotor advance ratio
ρ	= fluid density
ψ	= rotor azimuth angle

Presented as Paper 89-1845 at the AIAA 20th Fluid Dynamics, Plasma Dynamics, and Lasers Conference, Buffalo, NY, June 12-14, 1989; received June 9, 1990; revision received Sept. 11, 1990; accepted for publication Sept. 16, 1990.

*Engineer, Aerodynamic Computational Methods. Member AIAA.
†Engineer, Aerodynamics.
‡Research Scientist. Member AIAA.

Introduction

THE problem of high-speed forward flight is not new to the helicopter industry. For many years designers have tried to increase the maximum speed of the helicopter without incurring significant penalties in terms of vibration levels, required power, performance, etc. Unfortunately, much of the problem lies in the complexity of the helicopter's aerodynamic environment. In hover, each individual airfoil section of a rotor blade assumes a relatively constant angle of attack to the oncoming airflow as it passes around the azimuth. As cyclic pitch is introduced to the individual blades and the helicopter begins to move forward, a disparity arises over the rotor disk as to the relative fluid velocities present at each spanwise section and at each azimuthal position of the blade. The helicopter's forward flight speed adds to the rotational speed of the rotor on the advancing side of the disk and subtracts from it on the retreating side, and so as the forward flight speed increases, the disparity between the maximum fluid velocity on the advancing side and the minimum fluid velocity on the retreating side grows larger. At forward flight speeds near 200 kt, the maximum oncoming Mach number at the tip of the rotor can vary from 0.2 to 0.97 in one rotor revolution. The consequence of this rapid variation in fluid velocities encountered by the blade is that the angle of attack of the retreating side must be kept high, whereas that of the advancing side must be low. Only in this way is the lift distribution across the rotor disk established to trim the rotor rolling moment. This basic observation can serve as a guideline for the extension of the forward flight envelope if it is restated in the following manner: 1) design a rotor blade that will perform well at low angles of attack and high (transonic) Mach numbers, and 2) enable the same blade to perform well at high angles of attack and low Mach numbers.

This poses an extremely difficult problem since design parameters and equations used to create blades with better transonic performance are very nearly antithetical to the design rules used to create better high-α blades. The system

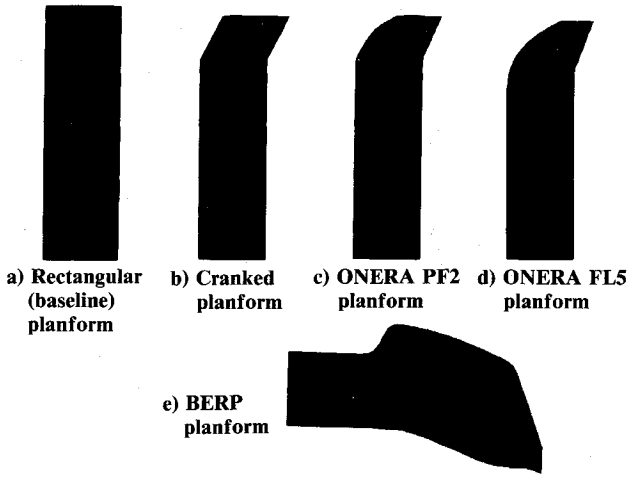

Fig. 1 Tip shapes used in computational study.

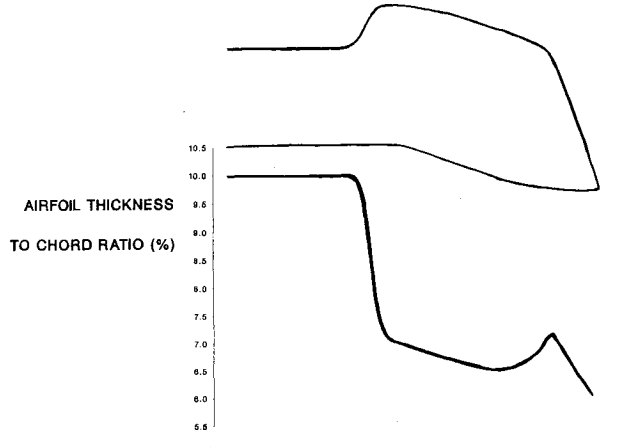

Fig. 2 Spanwise t/c variation for modified BERP and modified rectangular tip shapes.

described in this paper uses two techniques for evaluating rotor tip planforms in two different flow regimes. A full-potential, rotor-frame code is used to analyze planform shape in the transonic advancing part of the disk, whereas the complementary testing of the high-α retreating-blade environment is accomplished in the wind tunnel. Rotor tips that perform well in the transonic regime are thus tested for their suitability in high-α flows, and vice versa, with the ultimate driving force being the development of a rotor tip with markedly better flight characteristics in both areas.

Approach—Computational

The computational method involved in the analysis of the high-speed rotor tips, known as the full-potential rotor (FPR) code, was written by Strawn, Bridgeman, and their colleagues.[1-3] This steady/unsteady finite-difference code solves the full-potential equation in strong conservation form and in rotor coordinates.

The following planforms were chosen for this computational study: a baseline (rectangular) tip, a simply swept (cranked) tip, the ONERA PF2 and FL5 tips,[4,5] and the British Experimental Rotor Program (BERP) tip.[6-8] Figures 1a-1e show the planform outlines for these five test articles. It should be noted that only the planform of the BERP tip has been used in this evaluation process. The actual airfoils used on the Westland BERP blade are proprietary and unavailable to the public. Further reference to the BERP tip in this paper will refer only to the planform shape of the blade.

A typical grid around one of the rotor tips was a stacked-O cylindrical mesh consisting of 80 wraparound by 40 spanwise by 24 normal nodes. This standard mesh was sized to facilitate faster turnaround under the available memory cap of a Cray X-MP supercomputer. The criterion for flow solution convergence was taken to be the reduction of the maximum field residual by four orders of magnitude. Steady-state solutions were converged at an azimuth of 0 deg (pointing away from and parallel to the freestream). After the 0-deg solution was derived, the solution advanced through 180 deg of unsteady motion. All of the cases used the flight conditions that are listed in Table 1 as input parameters. The 10% section above ensured that at the given flight conditions a strong shock would form on the blade surface and that significant differences in drag levels could then be deduced from among all of the blade tips.

Table 1 Flight conditions used as input parameters

Advance ratio	0.45
Rotational tip Mach number	0.636
Total tip Mach number at deg azimuth	0.922
Angle of attack	1 deg
Aspect ratio—whole blade	16
Aspect ratio—computational zone	5
Root airfoil section	NACA 64A-010

For the purpose of this study, airfoil sections are assumed to be constant along the span of each blade in order to maximize performance differences based solely on planform. In the cases of the PF2 and the FL5 tips, the restriction of constant t/c thins the blade in profile where the chord changes in length. For the double-swept BERP planform, keeping a constant t/c noticeably thickens the blade at the forward sweep break and thins it quickly near the tip. Since production blades are not made with such a locally thickened region, two more test cases were designed that tested the performance of a constant-thickness BERP blade. In one, the thickness of each individual airfoil section is scaled inversely with the local chord length so as to create a constant overall blade thickness. Where the local chord is longest, this procedure reduces the local airfoil to approximately 7% t/c. At approximately 0.46 of a root chord length inboard of the tip, the blade begins to taper down to a 6% airfoil at the tip. Thus, we obtain the t/c curve in Fig. 2 for the modified BERP tip, which is more in line with what we would expect a production blade to follow. To perform a direct comparison between the modified BERP tip and a baseline planform, this same t/c distribution was then installed on a rectangular blade. The resulting tip is called the modified rectangular in this study.

Results—Computational

Constant 10% t/c

The local oncoming Mach number at the leading edge of a rotor blade in forward flight effectively varies linearly with the

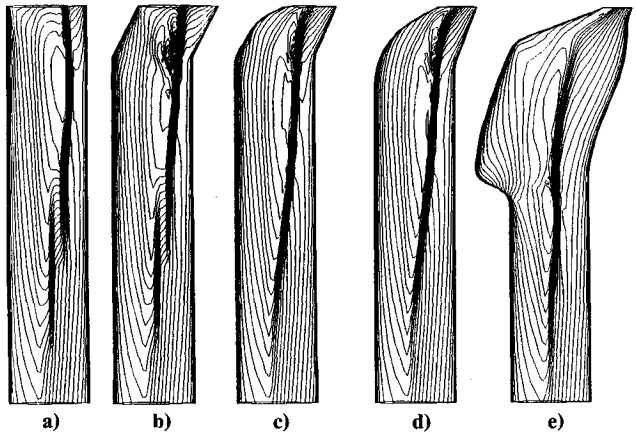

Fig. 3 Surface Mach number contours at 90-deg azimuth.

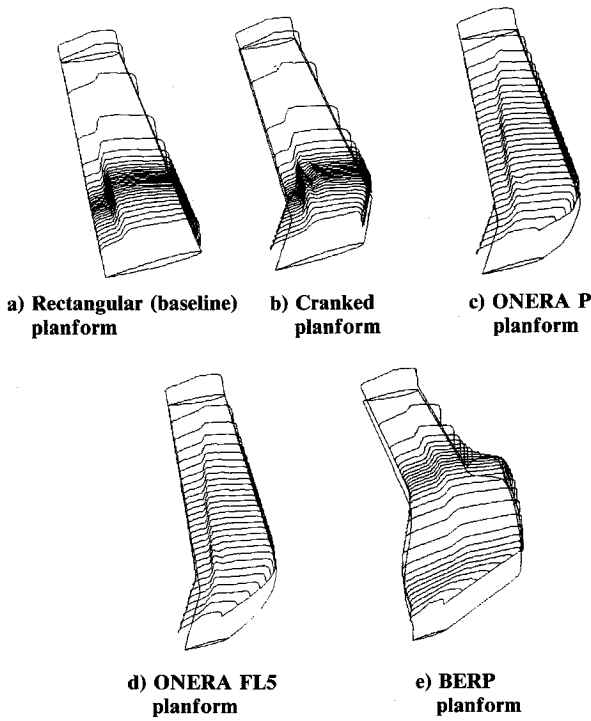

Fig. 4 Topographic presentation of Mach number on the blade surface at 90-deg azimuth.

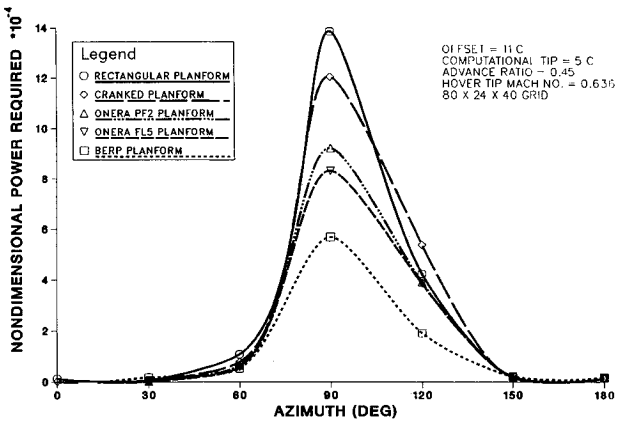

Fig. 5 Nondimensional power required to drive tip regions from 0-deg azimuth to 180 deg. Tip shapes have constant NACA 64A-010 airfoil sections.

span, therefore, any shocks that form tend to grow stronger toward the very tip of the blade. The results shown in Figs. 3 and 4 point out this phenomenon. The five blade tips with constant 10% airfoils are shown in both of these figures at 90-deg azimuth, where we would expect the overall shock strength to be the highest. As is shown in Fig. 3, Mach contours on the surface of the blades congregate at the shock, and the rectangular tip shows the strongest shock. Cranking the tip of the blade does reduce the strength somewhat, but not as much as continuously sweeping the leading and trailing edges. The PF2 and FL5 tips both lessen the shock strength appreciably over the outer two chords of the blade. The double-swept BERP planform, however, decreases the strength of the shock farther inboard than any single-swept tip. Figure 3 shows that the maximum Mach number on the surface of the BERP planform tip is lower than that found on any of the other tips and that the shock is diffused over the outer three chords of the blade.

Figure 4 shows three-dimensional views of the chordwise Mach contours along the surfaces of the blades. These contours are shown superimposed above a line drawing of each blade's planform for reference purposes. This topographic representation is well suited for pointing out the diffusion of the shock near the spanwise station of the BERP planform's forward sweep break. At these flight conditions, no other planform reduces the chordwise Mach number gradient and diffuses the shock so readily. Double-swept planforms such as the BERP tend to diffuse shocks by spreading the pressure recovery over a larger chordwise extent than the other blade tips.

In this study of constant t/c tip shapes, planform sweep effects are independent of airfoil type and depend only on flight condition. Therefore, we may use required power as the dependent variable in a parametric study of the planforms. To obtain a measure of required power, spanwise C_D values output by FPR were integrated and nondimensionalized according to the following equation:

$$\tilde{P}_{0_{\text{tip}}} = \frac{P_{0_{\text{tip}}}}{\frac{1}{2}\rho\alpha^3 R c_{\text{root}}} = \left(M_{\text{rot}_{\text{tip}}}\right)^3 \int_{0.6875}^{1.0} C_D(x)\tilde{c}(x)[x + \mu \sin\Psi]^3 \, dx$$

where

$$\tilde{c}(x) = c(x)/c_{\text{root}}$$

The integration is carried out from the inboard computation boundary ($r/R = 0.6875$) to the end of the blade ($r/R = 1.0$). The variations in $\tilde{P}_{0_{\text{tip}}}$ around the advancing side of the disk for all of the planforms are plotted against one another in Fig. 5. It is important to remember that this plot only displays the relative benefit of a reduction in wave and induced drag and does not consider skin friction (profile) drag. In general, the tips fall into a monotonic series, which points out the relative benefits of traditional transonic planform design quite clearly. The 90-deg azimuth shows more required power than any other azimuth in all cases. In addition, all of the rotor tips require more power in the forward half of the advancing side than at the rear. This is due to the delay of shock collapse after its initial formation. Just as traditional transonic theory dictates, a simple cranked tip performs better than a rectangular one. In addition, the drag peak of the cranked tip is shifted slightly toward the forward quadrant of the disk. This is a general result of simply swept planforms. The shock formation on the outboard crank is delayed until later in the azimuth range, where the incoming Mach number is decreased by the cosine of the advance ratio. The effect is most obvious when the crank consists of a single-sweep angle (in this case 23.5 deg).

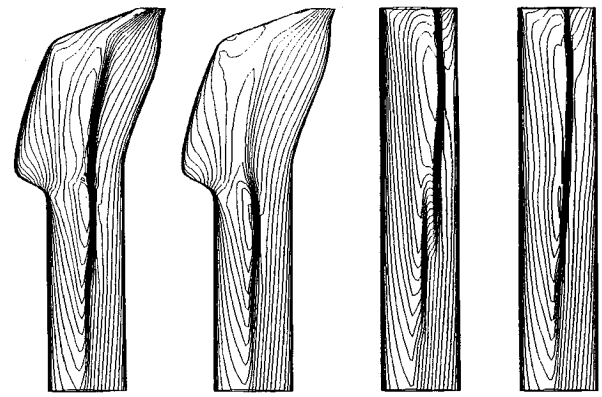

Fig. 6 Surface Mach number contours at 90-deg azimuth.

The tapered and more highly swept outer portion of the ONERA PF2 tip decreases the power required significantly more than does the cranked tip. A transition to the continuously swept leading edge of the FL5 tip drops the power even more. Of most importance is the trend of the bottom curve on the plot, where the BERP planform shows significantly lowered power requirement through the 90–120 deg range. As an example of a quantitative measure, the power required by the BERP tip is only 41% of that required by the rectangular tip at the 90-deg azimuth.

Modified *t/c* Variation

In general, the thinning of outboard sections on any rotor blade helps transonic performance by lessening the probability that shocks will arise. This phenomenon is shown graphically in Fig. 6, where side-by-side comparison can be made between the constant 10% *t/c* blades and the modified blades. The thinned sections serve to diffuse the shock farther inboard on the BERP planform and to lessen the overall shock strength on the rectangular planform. Both shocks have also moved forward slightly on their respective blades. As Fig. 7 shows, the values of required power are lowered dramatically. In fact, the gain in power that is made by going to the BERP planform from the square tip may be realized simply by adjusting the square tip's *t/c* distribution. In addition, the improvement made by a modification to the BERP planform's *t/c* distribution is not equal to that for the rectangular tip. Whereas the BERP planform required 41% of the power of the rectangular tip when a constant 10% airfoil was used, the modified BERP required 66% as much power as the modified rectangular blade. The rise is due to the reduction in shock strength and

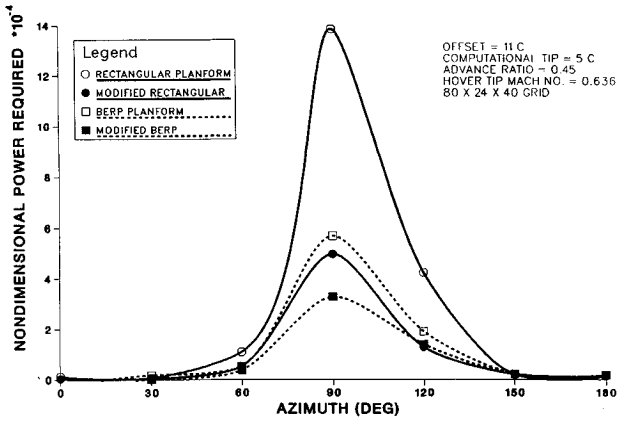

Fig. 7 Nondimensional power required to drive tip regions from 0-deg azimuth to 180 deg. Tip shapes have both constant and modified *t/c* distribution.

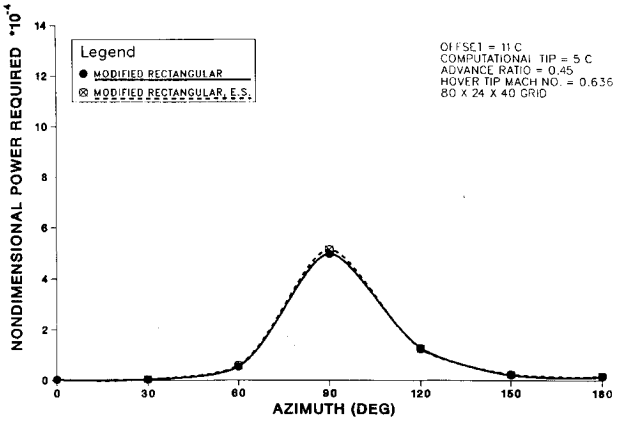

Fig. 8 Nondimensional power variation due to equalization of rectangular blade's thrust-weighted solidity to that of the BERP planform.

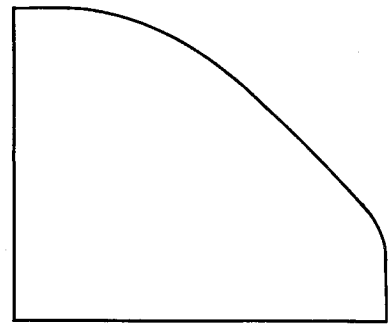

Fig. 9 Bell Helicopter's hyperbolic tip.

the more favorable placement of the shock, both resulting from the use of thinner sections.

The overall observations can be summed up as follows: 1) all blades can be adjusted to have markedly lower power requirements on the advancing side of the disk by thinning the sections, 2) transonic power requirements of double-swept tips such as the BERP tip are lower than those of rectangular or simply swept tips with the same *t/c* distribution, and 3) this advantage tends to lessen as shock strength decreases.

Solidity Considerations

Recent discussions about the performance of the BERP tip[13,14] have centered on the method of calculating the solidity of the blade. Essentially, if the root chord of the BERP tip shape is equal to the root chord of a baseline blade, then its nominal solidity is the same, but its thrust-weighted solidity is higher. This is essentially because more thrust is carried by the area toward the tip of a rotor blade. However, with an increase in the chord length of the rectangular blade, the thrust-weighted solidity can be increased up to that of the BERP blade. By our calculations, for an aspect ratio 16 blade, the chord must increase by 12.3%. If this change is made, the power required to drive the outer five chords of the blade increases slightly, as is shown in Fig. 8. But this change in chord has a relatively weak effect, compared to the sectional changes discussed earlier or the planform variation. We conclude that the equalization of the thrust-weighted solidity between two blade tip planforms has only a very small effect on the transonic wave drag levels measured around the advancing part of the disk.

Approach—Experimental

The hyperbolic tip shape (Fig. 9) was designed in the early 1970s as a simply swept alternative to rectangular rotor tip planforms.[9] Lift and drag characteristics of the hyperbolic tip were markedly better than those of rectangular tips in experimental studies.[10] Recent wind-tunnel tests in the Texas A & M low-speed wind tunnel confirmed this superiority and obtained comparative data on the performance of the BERP planform in addition.[11,12] These tests were designed to simulate some of the characteristics of typical retreating blade flow, including large-scale separation and deep stall. The designs tested were the following.

1) A baseline rectangular blade tip with constant NACA 0012 airfoil section.

2) A blade made from the planform of the BERP tip, using a NACA 64A-010 airfoil as root section and the modified *t/c* distribution shown in Fig. 2.

3) The Bell "hyperbolic" tip shape, using a constant NACA 0012 airfoil section.

The tests, which used the three blades listed above, consisted of the following.

1) Force and moment data in body-axis and wind-axis coordinate systems at $Re = 1.20 \times 10^6$ ($M = 0.13$). Angles of attack ranged from -2 to 22 deg. Yaw angles tested were 0, -20, and $+20$ deg.

2) Hot-wire anemometry data on wake structure behind blade tips at selected angles of attack and yaw angles.

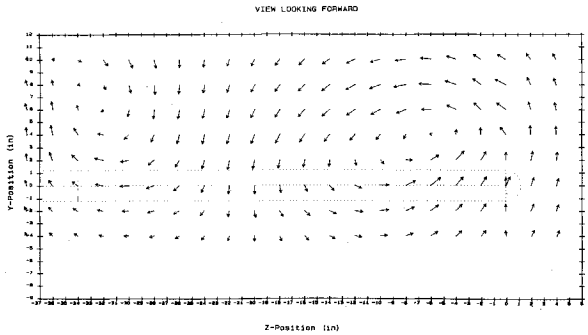

Fig. 10 Hot-wire anemometry study of velocity vectors in wake behind double-swept tip shape: $\alpha = 18$ deg (blade tip to right).

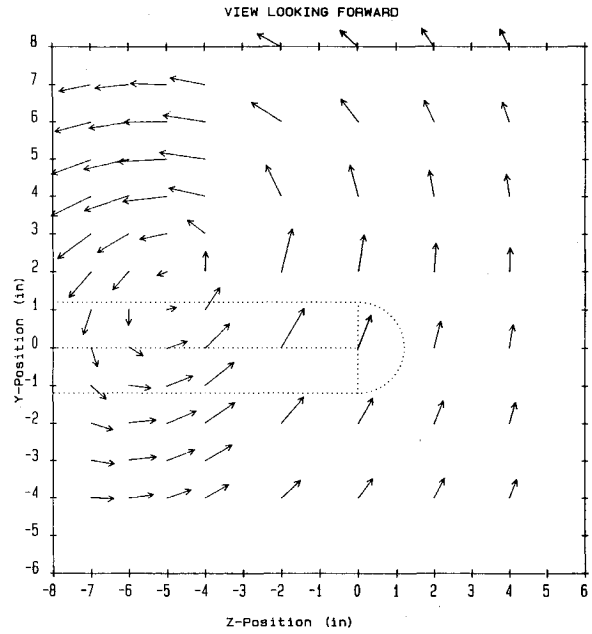

Fig. 11 Hot-wire anemometry study of velocity vectors in wake behind Bell Helicopter's hyperbolic tip shape: $\alpha = 18$ deg (blade tip to right).

3) Surface sublimation flow visualization, still pictures, and videos for most angles of attack and yaw angles.

4) Smoke visualization of most flow features at a reduced flow velocity ($Re = 1.25 \times 10^5$).

Quantitative measurements included force and moment data for all blade tips at all angles of attack. Data was taken at all yaw angles. Hot-wire anemometry of wake planes behind the blades outlined in a quantitative fashion the structure of the flow past the tips at several angles of attack and yaw angles. All flow visualization techniques were used to qualitatively evaluate separation, vortical structure, and reversed flow regions.

Results—Experimental

The existence and placement of vortices on the upper surfaces of the tested planforms were confirmed by hot-wire anemometry and flow visualization. Various techniques confirm that an inboard vortex forms at the forward sweep break of the BERP planform at moderate-to-high angles of attack. This phenomenon is shown graphically in Fig. 10, which is a perpendicular slice through the wake approximately one root chord downstream of a double-swept planform at $\alpha = 18$ deg. The outboard (or tip) vortex is relatively stronger than the inboard vortex and is of the opposite rotational sense. By comparison, hot-wire slices aft of the hyperbolic tip reveal a relatively stronger tip vortex, such as that shown in Fig. 11.

Combining the results of flow visualization with the hot-wire data, we can describe some major components of the fluid flow around the BERP and other double-swept planforms at high α. As Fig. 10 shows, two counter-rotating vortices form at the leading edge of the blade, one at the forward sweep break and one at the tip. The rotational sense of the vortices, as shown in Fig. 12, is such that downwash is induced over the paddle part of the planform between the vortices. This downwash energizes the boundary layer and reduces the local angle of attack seen by the outboard portion of the blade. Thus, the flow over the blade between the two vortices is braced and remains attached at higher α than it would if the vortices were not present. The corollary to this rule also holds: the flow inboard of the forward sweep break is more likely to separate because of the presence of the nearby vortex. Both of these traits are readily apparent in the oil flow traces in Fig. 13. This photo was taken at $\alpha = 16$ deg. Below the forward sweep break, the flow separates massively, and a large reverse flow pocket is created in the separated zone. Outboard of the sweep break the flow is attached. Near the tip, the large feather-shaped tip vortex is still attached to the surface. Tip vortices did not stay attached during the entire α sweep for any of the planforms tested. As a rule, the tip vortices lifted from the surface range from $\alpha = 16$ to 19 deg, with the BERP planform showing detachment at $\alpha = \sim 18$ deg. These phenomena were highly repeatable. Videotapes of the oil flow sublimation detail the order of events on the surface of the blade; attached vortical regions sweep oil along the

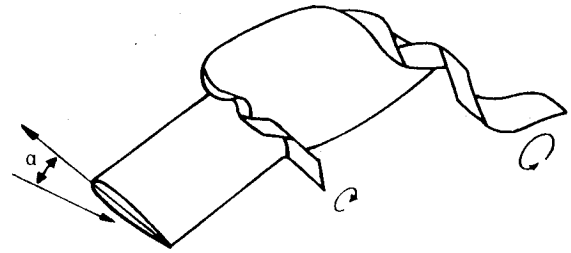

Fig. 12 Vortical flows for the BERP planform at high α.

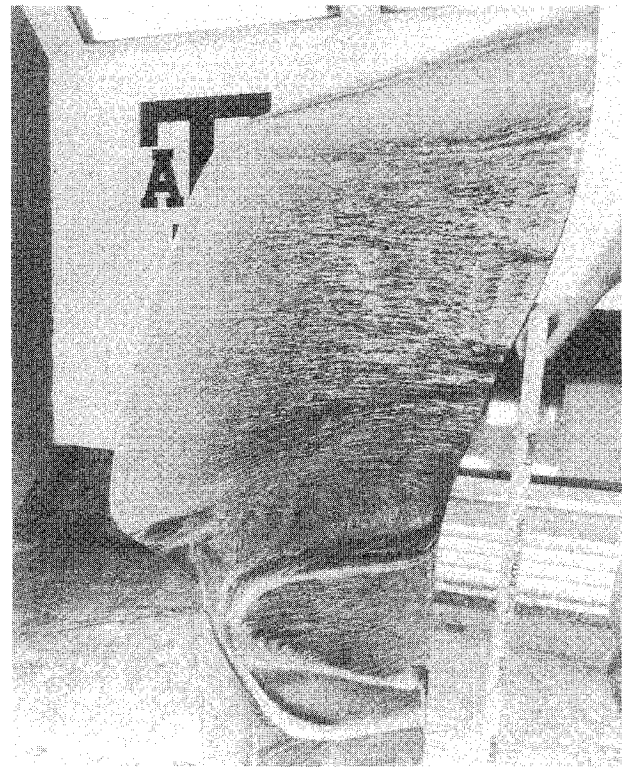

Fig. 13 Oil flow over BERP planform at $\alpha = 16$ deg, $Re = 1.20 \times 10^6$, $M = 0.13$.

surface quickly while slowly recirculating or separated areas tend to entrap large concentrations of the substance.

Some of the force and moment data of the advanced tip shapes are shown in Figs. 14–16. It is important to keep airfoil distinctions in mind when regarding these plots since the sectional distribution of the BERP tip as tested was drastically different from that of either of the other two blades. Both the rectangular and hyperbolic tip kept a constant NACA 0012 section, whereas the root section of the BERP tip was the thinner NACA 64-010 airfoil. The t/c distribution then followed that of the modified BERP tip shown in Fig. 2.

The C_L vs α curves in Fig. 14 show the characteristic hard stall of the rectangular blade as well as the tendency of the hyperbolic tip to soften and delay that stall. The BERP planform exhibits a strong tendency to avoid classical stall at high angles of attack. Instead of losing lift suddenly, the dual vortices allow the fluid between them to remain attached and the surface lifting over the range from $\alpha = 12$ to 22 deg. Figure 15 shows that one disadvantage of the BERP planform is the increased drag at high angles of attack. But we may also point out that L/D values are usually comparable to or better than those of rectangular blades. Further analysis of the C_L and C_D curves should be approached with caution because the thicknesses and airfoil types of the tested blades were unequal. For example, the early break in the BERP tip's C_D vs α curve may be due to the thin airfoil sections instead of the planform three-dimensional effect. But even so, the BERP planform,

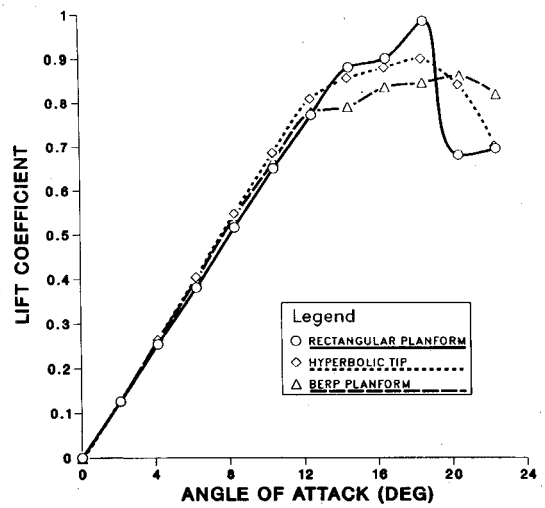

Fig. 14 Experimental C_L-α variation for three tip shapes: $Re = 1.20 \times 10^6$, $M = 0.13$.

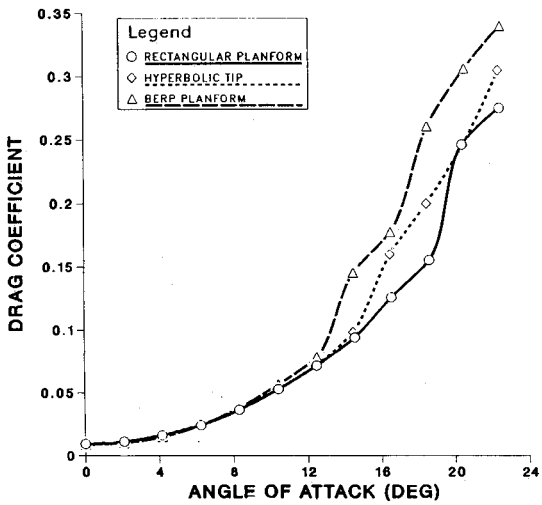

Fig. 15 Experimental C_D-α variation for three tip shapes: $Re = 1.20 \times 10^6$, $M = 0.13$.

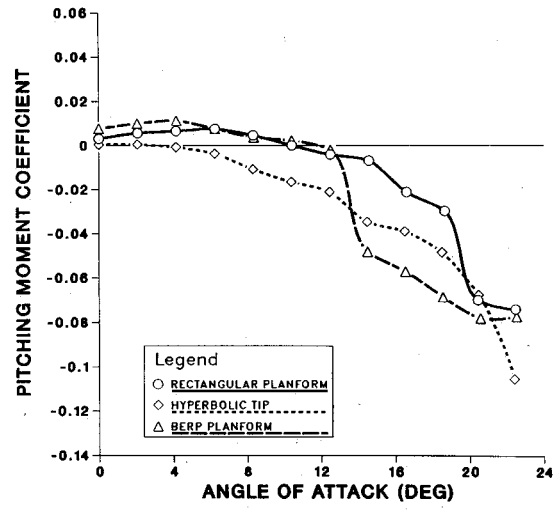

Fig. 16 Experimental C_M-α variation for three tip shapes: $Re = 1.20 \times 10^6$, $M = 0.13$.

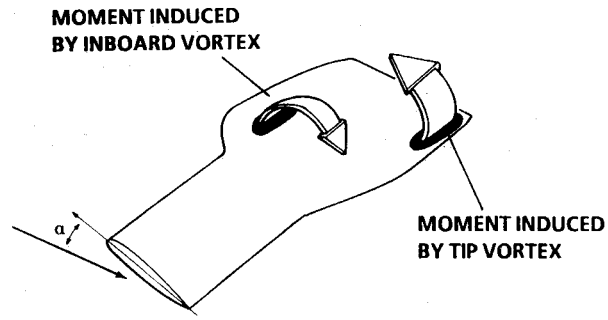

Fig. 17 Effective moment balance caused by vortex generation on BERP planform.

whose sections varied between 7 and 10% in thickness along the span, exhibited nearly the same C_L values as the thicker NACA 0012-based rectangular and hyperbolic planforms.

Helicopter designers are usually very interested in the pitching moment of a rotor blade since a host of aeroelastic and control problems can be linked to the C_M vs α curve. The trace of the rectangular blade in Fig. 16 is typical of the kind of results expected from simple, uncambered three-dimensional wings—a relatively flat C_M curve for most of the α sweep, followed by a decline into nose-down moment at high α. The hyperbolic tip deviates form this standard by allowing the strong tip vortex to stick to and interact with the relatively large tip area aft of its pitch-change axis. Even at low angels of attack, the suction of this vortex causes an overall nose-down moment, but at a relatively controllable constant slope. The BERP planform exhibits pitching characteristics somewhere between these two extremes. Like the rectangular tip's curve, the BERP planform's C_M curve stays close to zero moment through most of the linear regime. Between $\alpha = 12$ and 14 deg, the BERP planform breaks sharply and heads quickly into nose-down moment. This characteristic alone would tend to discourage the use of this particular planform shape since significant blade slap problems might arise on the retreating side. However, modification of key airfoil sections might alleviate the overall tendency of the blade to break over, thereby allowing its use again.

As they do for the hyperbolic tip, significant three-dimensional vortex effects come into play that tend to mediate the sharp decline of the BERP planform's C_M vs α curve. Suction caused by vortices acts in the forward-swept part of the blade as well as the rearward-swept portion. Since some suction is applied forward of the pitch axis of the overall blade, the resulting nose-up moment can be thought of as an inexpensive static balance to the nose-down moment created by vortex lift at the tip. This idea is shown schematically in Fig. 17. Though

the magnitudes of the forces and moments necessarily change with α, airfoil type, thickness, etc., this idea of static balance could explain some of the behavior of the BERP planform's pitching moment in Fig. 16. It is interesting to note that the characteristic break in the moment curve occurs 6 deg lower than the angle at which we see the tip vortex detach from the surface, which proves that the two phenomena are not causally related. However, the detachment of the forward sweep break vortex from the surface happens much earlier in the α sweep. When the vortex detaches, suction is no longer applied in the forward-swept region, the static moment "balance" is disrupted, and the attached tip vortex causes the entire tip region to pitch nose down. This scenario has the correct trend for the data and fits the observed flow visualizations.

Conclusions

The design of high-speed rotor tips can benefit from computational and experimental tests that directly compare performance characteristics of different planforms in realistic flight conditions. Computational results show that power required to drive rotor tips of constant t/c around the advancing side of the disk can be lowered significantly if planform design effectively manipulates the placement and strength of shocks on the tip surface. In particular, we find that the double-swept BERP planform is especially proficient at shock diffusion and can show a reduction in required power over rectangular or simply swept planforms with the same t/c variation. One specific sectional taper tested showed power reduction on the same order as the planform variation, and the combination of the two procedures yielded the most efficient blade.

At the other extreme of the rotor tip flight envelope, experimental tests show the BERP planform to be resistant to the hard stall usually seen with rectangular three-dimensional wings. Flow visualization studies coupled with examination of the force and moment curves point to a mechanism involving counter-rotating vortices of unequal strength that form at the forward sweep break and at the blade tip. Lift augmentation past stall is indicated as a byproduct of the induced downwash, and this hypothesis has been proven by hot-wire and surface sublimation studies. The test results show that higher drag levels accompany the BERP planform as α increases, yet the pitching moment behaves like that of a rectangular blade over a good portion of the α range. In any case, the BERP tip's moment curve falls between the curves of two tips that are both currently in production. Breaks in the moment curve as well as overall transonic drag levels could be improved by judicious selection of airfoil sections. In general, these results indicate that we can tune the forward-swept portion of a generic double-swept tip shape by controlling the amount of area forward of the pitch axis, the airfoils used, the forward and rearward sweep rates, etc. Such a tuned blade tip could ameliorate the traditional control, vibration, and aeroelastic problems that are usually assumed to accompany the use of swept rotor tips.

Overall evaluation must weigh the two regions of the rotor disk equally. The transonic performance of the BERP planform, as proven by this study, is slightly better than that of rectangular or simply swept tips when all blades have the same t/c distribution. Sectional taper may also be used to reduce transonic drag levels on rotor blades, and in this study, the modified rectangular blade requires essentially the same power as does the constant 10% t/c BERP planform. This result is significant because it shows two different methods for arriving at the same power requirements: planform variation (no taper) and sectional taper (constant planform). Most important, the benefits of these two methodologies appear to be cumulative, in the sense that the most significant reductions in power are derived when the planform is changed to diffuse the shock and the sections are altered to reduce its strength.

If the benefits of taper vs planform are dubious on the advancing side, they would probably not be so on the retreating side of the rotor disk. The rectangular blade with BERP sectional taper would probably perform more poorly than the constant 10% t/c rectangular blade in regions where stall is likely, owing to the fact that thin sections experience separation more readily than thicker ones. The wind-tunnel studies show that a tradeoff must be made between C_L vs α performance, pitching moment, and drag if judgment is to be passed on the BERP tip at high angles of attack. If the sharp break in the moment curve can be lessened by airfoil design, then the driving consideration becomes lift, and that in turn is governed by maximum forward flight speed requirements. For a 200+kt helicopter, the blade tips would regularly experience poststall angles of attack, and so the use of the BERP tip could be warranted. For slower helicopters, whose retreating blades do not experience massive stall, advantages are more dubious. For helicopters whose maximum forward flight speed is on the order of 170–180 kt, a simply swept tip such as the hyperbolic, the PF2, or the FL5 may provide efficient transonic relief while not penalizing the pitch dynamics of the retreating blade. In any case, tradeoffs remain a key element of the overall high-speed rotor tip design process. Coupling the advantages of sectional design to the problems of lowering transonic drag and relieving sharp breaks in moment curves could be a very effective method for better double-swept rotor tip design in the future.

Acknowledgments

Bell Helicopter Textron, Inc. would like to acknowledge the support and help of W. J. McCroskey of the U.S. Army Aeroflightdynamics Directorate—AVSCOM at NASA Ames Research Center.

References

[1]Bridgeman, J. O., Strawn, R. C., and Caradonna, F. X., "An Entropy and Viscosity Corrected Potential Method for Rotor Performance Prediction," *Proceedings of the 44th Annual National Forum of the American Helicopter Society,* Washington, DC, June 1988.

[2]Bridgeman, J. O., Steger, J. L., and Caradonna, F. X., "A Conservative Finite-Difference Algorithm for the Unsteady Transonic Potential Equation in Generalized Coordinates," AIAA Paper 82-1388, Aug. 1982.

[3]Strawn, R. C., and Caradonna, F. X., "Conservative Full Potential Model for Unsteady Transonic Rotor Flow," *AIAA Journal,* Vol. 25, No. 2, 1987, pp. 193–198.

[4]Guillet, F., and Philippe, J., "Flight Test of a Sweptback Parabolic Tip and a Dauphin 365N," Office National d'Etudes et de Recherches Aérospatiales TP-1984-84, Aug. 1984.

[5]Desopper, A., "Study of the Unsteady Transonic Flow on Rotor Blade with Different Tip Shapes," Office National d'Etudes et de Recherches Aérospatiales, TP-1984-82, Aug. 1984.

[6]Perry, F. J., "Aerodynamics of the Helicopter Speed Record," *Proceedings of the 43rd Annual National Forum of the American Helicopter Society,* St. Louis, MO, May 1987.

[7]Wanstall, B., "BERP Blades: Key to the 200-Knot Helicopter," *Interavia,* March, 1986, pp. 322–324.

[8]Hopkins, H., "Fastest Blades in the World," *Flight International,* Dec. 1986, pp. 24–27.

[9]Spivey, W. A., and Morehouse, G. G., "New Insights into the Design of Swept-Tip Rotor Blades," *Proceedings of the 2nd Annual National Forum of the American Helicopter Society,* Washington, DC, June 1970.

[10]Drees, J. M., "High-Speed Helicopter Rotor Design," *Proceedings of the 19th Annual National Forum of the American Helicopter Society,* Washington, DC, 1963.

[11]Sigl, D. G., "Tabulated Wind Tunnel Test Results for SHARC, BAHR, BERP, Hyperbolic, and Rectangular Tips," Bell IOM 81:DGS:lre-1789, March, 1989.

[12]Pirkle, P. S., "Main Rotor Tips Study (Continued) for Bell Helicopter Textron, Fort Worth," Aerospace Engineering Department, Texas A & M University, College Station, TX, Rept. TR-8827, Oct.-Nov. 1988.

[13]Amer, K. B., "High Speed Rotor Aerodynamics," *AHS Journal,* Vol, 34. No. 1, 1989, p. 63.

[14]Perry, F. J., "The Contribution of Planform Area to the Performance of the BERP Rotor," *AHS Journal,* Vol. 34, No. 1, 1989, pp. 64–65.